Atmos. Meas. Tech. Discuss., 5, 3431–3471, 2012
www.atmos-meas-tech-discuss.net/5/3431/2012/
doi:10.5194/amtd-5-3431-2012

Atmospheric Measurement Techniques Discussions

Investigating the long-term evolution of subtropical ozone profiles applying ground-based FTIR spectrometry

O. E. García[1], M. Schneider[2,1], A. Redondas[1], Y. González[1], F. Hase[2], T. Blumenstock[2], and E. Sepúlveda[3,1]

[1]Izaña Atmospheric Research Centre (IARC), Agencia Estatal de Meteorología (AEMET), Santa Cruz de Tenerife, Spain
[2]Institute for Meteorology and Climate Research (IMK-ASF), Karlsruhe Institute of Technology (KIT), Karlsruhe, Germany
[3]University of La Laguna, La Laguna, Spain

Received: 9 February 2012 – Accepted: 21 March 2012 – Published: 10 May 2012

Correspondence to: O. E. García (ogarciar@aemet.es)

Published by Copernicus Publications on behalf of the European Geosciences Union.

Abstract

We investigate the long-term evolution of subtropical ozone profile time series (1999–2010) obtained from different ground-based FTIR (Fourier Transform InfraRed) retrieval setups. We examine the influence of an additional temperature retrieval and different constraints. The study is performed at the Izaña Observatory ozone super-site (Tenerife Island, Spain). The FTIR system is able to resolve four independent ozone layers with a theoretical precision of better than 7.5 % in the troposphere, lower, middle and upper stratosphere. This total error includes the smoothing error, which is dominating the random error budget. Furthermore, our theoretical calculations indicate that a very precise knowledge of the instrumental line shape is mandatory for a precise ground-based FTIR remote sensing of stratospheric ozone. Likewise, we show that a simultaneous temperature retrieval is highly recommended. We empirically confirm our precision estimates by daily intercomparisons with Electro Chemical Cell (ECC) sonde profiles. Both FTIR and ECC sonde profile time series show similar seasonality: in winter stratospheric ozone profiles are typical middle latitude profiles (low tropopause, low ozone maximum concentrations) and in summer/autumn they are typical tropical profiles (high tropopause, high maximum concentrations). Good agreement is also observed for the linear trends estimated from the FTIR and the ECC datasets: a negative trend in the upper troposphere/lower stratosphere region of about $-0.3\,\%\,\mathrm{yr}^{-1}$ and a positive trend in the middle/upper stratosphere of about $+0.3\,\%\,\mathrm{yr}^{-1}$. Admittedly, a 12-yr time series is too short for reliable trend studies, however, it is worthwhile mentioning that such subtropical ozone profile trends are predicted by climate models due to an increased stratospheric circulation in response to climate change.

AMTD

5, 3431–3471, 2012

1 Introduction

In the coming decades some kind of ozone recovery is expected, however, it is difficult to predict how, when, and to what extent it will occur (Weatherhead and Andersen, 2006). Currently it is discussed how climate change will interact with ozone recovery. Climate models predict an accelerated stratospheric circulation, leading to changes in the spatial distribution of stratospheric ozone and an increased stratosphere-to-troposphere ozone flux (Hegglin and Shepherd, 2009, and references therein). In order to verify or decline the different climate model simulations consistent long-term observations of the vertical distribution of ozone are required. Since the expected signals are rather small (e.g. expected trends from −3 % to +1 % per decade between 1960 and 2100 Hegglin and Shepherd, 2009; Li et al., 2009), only high precision observational datasets are useful.

Analyzing high quality ground-based solar absorption spectra in the mid infrared region (950–1050 cm^{-1}) yields high quality ozone total amounts (Schneider and Hase, 2008; Schneider et al., 2008a; Viatte et al., 2011) and profiles (Schneider et al., 2008b). Such infrared spectra have been measured by ground-based FTIR (Fourier Transform InfraRed) spectrometers for up to two decades at globally distributed sites within the NDACC (Network for the Detection of Atmospheric Composition Change, e.g. Kurylo and Zander, 2000; Vigouroux et al., 2008).

The FTIR ozone data are very interesting for validating climate model simulations, but it is important to apply a retrieval setup that best assures the high quality of the profiles. Furthermore, it is important to document that the high quality can be maintained over many years. Only very consistent and high quality long-term time series are useful.

In this work we present different FTIR ozone profile retrieval setups and perform a detailed theoretical and empirical FTIR data quality documentation. The study is performed for the ozone super-site Izaña Observatory, where since 1999 the FTIR measurements have been performed in coincidence to several other high quality atmospheric ozone measurement techniques (e.g. Brewer spectrometer, Electro Chemical

AMTD
5, 3431–3471, 2012

Cell, ECC, sondes, photometric in-situ surface). The Izaña Observatory and its Ozone Programme is described in Sect. 2, while in Sect. 3 the FTIR retrieval strategy is shown. In Sects. 4 and 5 we show the consistency and quality of the ECC sonde and FTIR data, and in Sect. 6 we present the ozone trend and seasonality in different layers. Finally, the main results are summarized in Sect. 7.

2 The Izaña observatory and its ozone programme

The Izaña Observatory (28.3° N, 16.5° W) belongs to the Spanish Meteorological Agency (AEMET). It is a subtropical high mountain observatory, located at 2.37 km altitude on Tenerife Island, and above a temperature inversion layer acting as a natural barrier for local pollution. Hence, it offers excellent conditions for the remote sensing of the upper atmosphere.

Since many years the Izaña Observatory has been a WMO/GAW (World Meteorological Organisation/Global Atmospheric Watch) station and an NDACC site, monitoring a large variety of atmospheric constituents, among them, ozone total amounts and ozone profiles. Different ozone measuring techniques are applied: Brewer spectrometer, FTIR spectrometer, Differential Optical Absorption Spectroscopy (DOAS), in-situ ultraviolet photometric analyzers, and ECC sondes. In this study we focus on ozone profiles and in the following two subsections we briefly describe the techniques that can measure ozone concentrations at different altitudes above the Izaña Observatory.

2.1 FTIR programme

Ground-based FTIR systems measure solar absorption spectra applying a high resolution Fourier Transform spectrometer. The FTIR activities at Izaña started in 1999 when, in the framework of a collaboration between AEMET and KIT (Karlsruhe Institute of Technology, Germany), a Bruker IFS 120M was installed at the Observatory. In January 2005 KIT scientists substituted this spectrometer by a Bruker IFS 120/5HR,

AMTD
5, 3431–3471, 2012

which is one of the best performing FTIR spectrometers commercially available. During March and April 2005 both instruments measured side-by-side, which allows for documenting the consistency of both FTIRs.

Since 1999 the Izaña experiment provides data to the NDACC network. Currently there are about 25 ground-based FTIR NDACC experiments. For NDACC, the solar absorption spectra are measured in the middle infrared spectral region (between 740 and 4250 cm^{-1}, which corresponds to 13.5 and 2.4 µm). At Izaña the FTIR spectra are measured on two or three days per week, with a high spectral resolution of 0.005 cm^{-1} (maximum optical path difference, OPD_{max} of 180 cm).

2.2 ECC and in-situ surface programme

The ozone sonde programme on Tenerife started in November 1992 and since March 2001 these ECC sonde activities form part of the NDACC. The sondes (type: Scientific Pump 6A) are launched weekly very close to the Izaña Observatory: from Santa Cruz de Tenerife (35 km northeast of the Observatory) and since October 2006 from Güímar (15 km east of the Observatory). Smit et al. (2007) demonstrate that the expected uncertainty of these ECC sonde profiles is ±5–10 %.

Since 1987, and in the framework of the GAW programme, in-situ surface ozone has been monitored. During this period, different ultraviolet absorption instruments have been applied. Since 1999, two TEI analyzers (Thermo Electron corporation environmental Instruments) are in operation. They continuously record one-minute average ozone values. Zero-checks with an activated-carbon absorber are performed on a daily basis to detect instrumental offset drifts. This surface ozone programme has been audited by the World Calibration Centre for Surface Ozone, Carbon Monoxide and Methane each two or four years since 1996. The expected uncertainty is to be ±1 ppb (Zellweger et al., 2009).

At the Izaña high altitude Observatory the surface measurements are well representative of the free troposphere and, thus, are well suited for validating the tropospheric ozone concentrations observed by the FTIR system (see also Sepúlveda et al., 2012).

AMTD
5, 3431–3471, 2012

3 Ground-based FTIR ozone measurements

3.1 Ozone retrieval strategy

The high resolution spectra allow an observation of the pressure broadening effect, and thus, the retrieval of trace gas profiles. The inversion problems faced in atmospheric remote sensing are in general ill-determined and the solution has to be properly constrained. An extensive treatment of this topic is given in the textbook of C. D. Rodgers (Rodgers, 2000).

We apply the retrieval code PROFFIT (Hase et al., 2004) for retrieving the FTIR ozone profiles and investigate three different retrieval setups (in the following referred as retrieval setups A, B and C, see Table 1). All setups apply the spectral ozone microwindow suggested by Barret et al. (2002) (see Fig. 1) and the different ozone isotopologues ($^{666}O_3$, $^{686}O_3$ and $^{668}O_3$) are retrieved on a logarithmic scale. Setup A is the less sophisticated setup and it can be considered as the "NDACC" approach except for the logarithmic instead of the linear scale retrieval of ozone. Setup B is further refined by an additional temperature retrieval, for which we simultaneously fit four CO_2 microwindows between 962 and 970 cm^{-1} (Schneider and Hase, 2008). For these two setups the inversion problem is solved using an ad-hoc Tikhonov-Phillips (TP) slope constraint (TP1 constraint). Finally, the setup C is further refined by applying an Optimal Estimation (OE) constraint instead of the ad-hoc TP1 constraint. In this case, the a priori covariance matrix, $\mathbf{S}_a$, is taken from an ECC sonde climatology calculated from measurements between 1996 and 2006 (Schneider et al., 2008b). In addition setup C includes an inter-species constraint between the different ozone isotopologues ($^{666}O_3$, $^{686}O_3$ and $^{668}O_3$, Schneider et al., 2006). Setup C can be considered as the optimal setup, since the actual covariances of ozone and of the different ozone isotopologues is taken into account.

For all setups H_2O, CO_2 and C_2H_4 are considered as main interfering absorbers. Spectroscopic line parameters are taken from the HITRAN 2008 database (Rothman

AMTD
5, 3431–3471, 2012

et al., 2009), expect for H_2O, where the parameters from the HITRAN 2009 update are applied.

The a priori mean profiles are taken from the WACCM climatology (Whole Atmosphere Community Climate Model, http://waccm.acd.ucar.edu) provided by James W. Hanningan (National Center for Atmospheric Research). As a priori for the ozone isotopologue ratios we assume a heavy ozone enrichment of 100 % throughout the atmosphere. It is important to mention that we do not vary our a priori depending on season. Thereby all variability observed in our retrieved profiles comes from the measurements.

As a priori temperature we use the diurnal radiosondes (Vaisala RS92) up to 30 km and extended it by the NCEP (National Centers for Environmental Prediction) 12:00 UT daily temperature profiles. The radiosondes are launched twice per day (23:15 UT and 11:15 UT), just about 15 km southeast of the Izaña Observatory on the coastline.

3.2 Vertical resolution of FTIR ozone profiles

The vertical structures that are detectable by a ground-based FTIR system are given by the averaging kernel matrix (avks, $\hat{\mathbf{A}}$). The columns of this matrix are displayed in Fig. 2 for a typical measurement of the spectrometer 120/5HR and for the setups B and C (the avks of setup A are similar to the avks of setup B). The different widths of the avks and the different sensitivities (sum along the row of the avks) is mainly due to the differences in the applied a priori constraint. For all setups and for altitudes below 40 km the sensitivity is better than 80 %. Beyond 40 km the sensitivity significantly decreases for setup C.

Following Rodgers (2000), the number of independent layers of a retrieved gas profile can be quantified by the number of degrees of freedom for signal (dof). The dof is the trace of the averaging kernel matrix. For ozone, a mean total dof of around four is observed for all setups (see Table 2), meaning that the FTIR system is able to resolve four independent atmospheric layers: the troposphere (2.37–10 km), the tropopause region (11–21 km), the lower/middle stratosphere around the ozone maximum (22–29 km), and the middle/upper stratosphere (31–42 km). We have highlighted the ozone

AMTD
5, 3431–3471, 2012

kernels at the altitudes of 5, 18, 29 and 39 km in representation of these layers (see Fig. 2). The influence of the retrieval settings is also visible in the dof: for setup C the dof below 31 km is higher if compared to the setups A and B. Up to 31 km the setup C profiles have a better vertical resolution than the setup A and B profiles. This is a consequence of the rather loose constraint applied for setup C at these altitudes (the constraint of setup C is based on real ozone data, which show high variabilities from 15 to 25 km due to a vertically shifting tropopause).

When interpreting the FTIR time series it is important to consider the time evolution of avks (Fig. 3 shows the time series of the total dof of setup C). We observe some kind of annual cycle in the dof time series. Furthermore, there is a jump when changing from the IFS 120M and IFS 120/5HR instrument. As expected, we observe that the dof obtained from IFS 120M spectra are smaller than the ones obtained from the IFS 120/5HR spectra: the total dof values differ by 7 %. This difference is smaller in the troposphere (6–7 %) than in the stratosphere (up to 10 %).

3.3 Error estimation

The error estimation is analytically performed by the retrieval code PROFFIT (Hase et al., 2004). It is based on the formalism suggested by Rodgers (2000). We consider three error types: (a) errors due to uncertainties in the input parameters (instrumental characteristics, spectroscopy data, etc.), (b) the smoothing error, and (c) errors due to measurement noise.

As uncertainties in the input parameters we assume the values as listed in Table 3. The uncertainties are split into statistical and systematic contributions, 80 % and 20 % respectively, except for spectroscopic parameters (line strength and pressure broadening coefficient), for which the entire uncertainty in the input parameter is systematic. The assumptions of Table 3 are reasonable for the IFS 120/5HR, but are very likely too optimistic for the IFS 120M (see for instance the discussion in Sect. 3.4). Hence, Table 3 only describes the errors for the IFS 120/5HR. For the IFS 120M the errors due to measurement noise, LOS (Line of Sight) and ILS (Instrumental Line Shape:

AMTD
5, 3431–3471, 2012

interferometer's modulation efficiency and phase error) uncertainties are by a factor of 2–3 larger.

The propagation of uncertainty sources for a typical measurement of the spectrometer 120/5HR, and applying the different retrieval setups, is displayed in Fig. 4. The smoothing error, associated with the smoothing of the real vertical distribution of ozone by the FTIR measurement process, is the leading error for all setups. It reaches about 50 % in the tropopause region, where the ozone concentrations are very variable and the profile might be highly-structured. The FTIR system is not able to resolve such fine vertical structures. Excluding the smoothing error, below 20 km the random errors are dominated by the measurement noise, the temperature and the ILS uncertainties, being the total error lower than 1.5 % for the setups A and B. For setup C we observe maximum errors of 3 % for the layer between 10 and 18 km. However, in this context it has to be noted that the profiles produced by setup C are vertically higher resolved if compared to the profiles produced by the other retrieval setups (e.g. compare left and right panel of Fig. 2 and the dof values of Table 2). Above 20 km and for setup A the error due to temperature uncertainties notably increases, reaching about 5 % at 40 km. In contrast to the setups retrieving the temperature (setups B and C), where the respective errors are lower than 2.5 %.

Table 4 shows the random error budget for different partial column amounts. It lists the total random errors (TRE) estimated as the root-square-sum of all parameter errors (TPE, input parameters and measurement noise) and the smoothing error (SE): $\sigma_{\mathrm{TRE}} = \sqrt{\sigma^2_{\mathrm{TPE}} + \sigma^2_{\mathrm{SE}}}$. Applying the retrieval setup C, the FTIR technique provides ozone partial columns with an overall precision of better than 4 % for the tropopause and middle stratosphere and of better than 7.5 % for the troposphere and the midle/upper stratosphere.

Regarding systematic errors, the error profiles also depend on the applied retrieval setup. Regarding setup B and C the spectroscopic parameters are responsible for most of the systematic errors. However, for setup A the temperature uncertainty becomes an important systematic error source, especially above the tropopause region. This fact

AMTD
5, 3431–3471, 2012

illustrates that a simultaneous temperature retrieval is important when aiming at high quality middle stratospheric ozone data.

3.4 Long-term consistency

Figure 4 show that the ILS uncertainties are an important error source (in particularly in middle and upper stratosphere). When aiming on a consistent long-term quality of ozone profiles a continuous and precise documentation of the ILS is mandatory. Therefore, at Izaña we make regular low pressure N_2O cell measurements. These measurements allow for retrieving the actual ILS by means of the LINEFIT code (Hase et al., 1999). LINEFIT estimates the ILS at 20 equidistant optical path intercepts. At Izaña we have performed such cell measurements about every two months. Figure 5 shows the 1999–2010 time series of the modulation efficiency obtained for the two spectrometers. The jumps in the time series (beginning of 2005 for IFS 120M and June 2008 for the IFS 120/5HR) are due to realignments of the instruments.

As expected we observe that the ILS of IFS 120M is significantly less stable than the ILS of IFS 120/5HR. While for the IFS 120/5HR the modulation efficiency can be determined with a precision of about 1 %, for the IFS 120M we only achieve a precision of 3 %. Concerning the phase error we make a similar observation: with our regular cell measurements we can achieve a precision of 0.005 rad for the IFS 120/5HR, but only of 0.025 rad for the IFS 120M.

3.5 Comparison between IFS 120M and IFS 120/5HR

During March and April 2005 both instruments (IFS 120M and IFS 120/5HR) measured side-by-side. The comparison between these coincident measurements is displayed in Fig. 6, where the ozone partial columns retrieved using the setup C are shown.

The agreement is excellent, except for the highest layers, where the FTIR data are more sensitive to instrumental uncertainties (ILS and measurement noise, see Fig. 4). For example, we observe a mean ratio between the IFS 120/5HR and 120M data of

AMTD
5, 3431–3471, 2012

1.00 ± 0.00 with a correlation of 99 % in 2.37–11 km layer in contrast to 0.96 ± 0.01 with a correlation of 83 % in 31–42 km layer. Furthermore, we find more scatter and lower correlation coefficients at the highest altitudes when applying the less refined setups A and B. This is expected from the error estimation (see Table 5). Thus, a mean ratio of 1.01 ± 0.01 is found in 31–42 km layer for the setup A, but only with a correlation of 71 %. Note also that higher errors are expected for the 120M ozone retrievals due to its higher ILS uncertainties (see Fig. 5) and its higher measurement noise and, consequently, lower sensitivity. The lower sensitivity is clearly observed by comparing the dof time series of retrieved ozone from the two spectrometers (see Fig. 3).

4 Consistency of ECC sonde time series

Before assessing annual cycles and trends it is very important to check the consistency of the ozone time series. The ozone super-site Izaña Observatory and its special conditions provide an excellent opportunity for this issue, since there are many different techniques that monitor atmospheric ozone. In this section we use these coincident measurements for empirically documenting the quality and the long-term stability of the ECC sonde dataset.

4.1 ECC sonde vs. Brewer

The consistency and quality of ECC sonde ozone profile ($\boldsymbol{x}_{\mathrm{ECC\_org}}$) time series can be evaluated by comparing it to independent and coincident very high quality measurements of total ozone amounts. At the Izaña Observatory such high quality measurements are performed by the FTIR system and by Brewer spectrometers. The Brewers have been operative since May 1991, and like the ECC sonde and FTIR programmes, they are part of NDACC since March 2001. Furthermore, since November 2003 they represent the Regional Brewer Calibration Centre for Europe (http://www.rbcc-e.org/)

AMTD
5, 3431–3471, 2012

of WMO/GAW, which guarantees the high quality of their total ozone measurements (better than 1 %, Redondas and Cede, 2006).

The ECC sondes normally burst between 30 and 34 km. In order to homogenize the study we only consider the ECC data measured up to 31 km. Thus, the ozone total columns from the ECC sondes (TC_{ECC_org}) have been calculated by integrating the ozone profiles up to 31 km and adding a typical residual ozone column up to the top of atmosphere. This residual has been estimated from the mean difference between the daily Brewer total ozone columns (TC_{Brewer}) and ECC ozone partial amounts up to 31 km (PC_{ECC_org}) for all 459 Brewer/ECC coincidences from 1999 to 2010 (for more details see Schneider et al., 2008a). We found a mean and a standard deviation (1σ) for the ozone residual of 61.8 and 10.2 DU respectively.

The Brewer total ozone columns can be used to correct the ECC sonde profiles ($\boldsymbol{x}_{ECC}$) by:

$$\boldsymbol{x}_{ECC} = \frac{TC_{Brewer}}{PC_{ECC\_org} + 61.8} \cdot \boldsymbol{x}_{ECC\_org} = CF \cdot \boldsymbol{x}_{ECC\_org} \quad (1)$$

whereby CF ($CF = \frac{TC_{Brewer}}{PC_{ECC\_org} + 61.8}$) is the daily correction factor. Schneider et al. (2008a) illustrated that by this correction the quality of the ECC data can be significantly improved.

The CF time series is displayed in Fig. 7a. We observe a jump in 2005. In fact, the mean CF is 1.02 ± 0.03 and 0.98 ± 0.03 for the periods 1999–2004 and 2005–2010, respectively. Such systematic change of about −4 % between the ECC records can be expected by changing the sensing solution type or ECC sonde type (Smit et al., 2007, and references therein). During 2005 the sensing solutions in the ECC sondes were substituted by a new batch, but the same manufacturer's operating procedures, and ratio of cathode sensing solutions have been kept during whole period (1999–2010). Nonetheless, in the light of above results, we might assume that some change in the sensing solutions was introduced by using the new batch. The discontinuities in the CF time series is also identified by a rank order change point test (Lanzante, 1996;

AMTD
5, 3431–3471, 2012

Romero et al., 2011). This non-parametric method, based on the ranks of the monthly values from a time series, is not particularly affected by gaps and outliers in the time series.

The time series of ECC ozone total columns, without and with correction (TC_{ECC_org} and TC_{ECC}, respectively), is displayed in Fig. 7b. The corrected ECC records benefit from the synergies of the two techniques: the high vertical resolution of the ECC sondes and the high precision of the Brewer measurements.

4.2 ECC sonde vs. surface

As aforementioned, at the Izaña Observatory the tropospheric surface ozone is also monitored by photometric in-situ analyzers. Thus, this surface dataset can also be used for documenting the long-term consistency of the ECC sonde profiles at Izaña's altitude.

In order to evaluate possible drifts in the ECC sonde dataset we examine the time series of the monthly relative differences with regard to the photometric surface data (Fig. 8). To do so the photometric surface data were averaged 30 min around the ECC measurements. For the ECC data corrected according to Eq. (1), the drift, i.e. the trend in the differences, is not significant ($0.31 \pm 0.52\,\%\,yr^{-1}$). On average, we find a mean bias and a scatter (1σ) of 10 % and 15 % respectively between the two techniques. We think that these are acceptable values considering the large natural variability of the monthly mean of photometric surface data, 14 % (1σ).

Note that, if the ECC profiles are not corrected, we observed a significant drift in the ECC/surface difference time series ($0.94 \pm 0.51\,\%\,yr^{-1}$), indicating the importance of correcting the ECC time series before using it for long-term studies. The jump in the ECC time series clearly affects the estimated ozone trends as well as the intercomparison with another technique. Therefore, in the subsequent analysis we will exclusively apply the corrected ECC sonde time series (corrected according to Eq. 1).

AMTD
5, 3431–3471, 2012

5 Validation of FTIR ozone profiles

The corrected ECC sonde time series can be used for evaluating the quality of the FTIR ozone profiles. To do so we have to consider that the vertical resolution of the ECC sonde and the FTIR profiles are rather different. Therefore, we only compare the layers that are detectable by the ground-based FTIR system, i.e. the ozone partial columns for the layers 2.37–10 km, 11–21 km and 22–29 km. Since the ECC sonde profiles are not smoothed by the FTIR avks (e.g. Schneider et al., 2008b), the advantage of the improved vertical resolution observed for the more sophisticated retrieval setups can directly be validated. Likewise, not smoothing the ECC sonde data with the FTIR avks assures that both the FTIR and the ECC time series remain completely independent and, for instance, the ECC sonde trends are not influenced by possible trends of the FTIR avks (see Fig. 3).

The straightforward comparison of ozone partial columns from FTIR and corrected ECC sondes is rather satisfactory, as shown Fig. 9. We find a mean bias between −6 % and −3 % in troposphere (2.37–10 km) and tropopause region (11–21 km) and around 7 % in middle stratosphere (22–29 km) for all retrieval recipes, while the scatter is between 7 % and 10 % for the two first layers and only of 4 % in middle stratosphere (see Fig. 9a and b). These results rather agree with the expected uncertainty for the ECC sondes given by Smit et al. (2007) (±5–10 %) and with our FTIR theoretical error estimation (Sect. 3.3). Furthermore, they are in good agreement with other similar intercomparison studies (Calisesi et al., 2005; Nair et al., 2011 and references therein). It illustrates the good agreement between the ECC sonde and FTIR techniques. As example, Fig. 10 shows the direct comparison between the coincident FTIR (setup C) and ECC sonde partial columns from 1999 to 2010 ($N = 243$).

The smoothing error might explain a large part of the discrepancy between FTIR and ECC sonde measurements (recall Table 4), although other sources of discrepancy should be considered like the observation of different airmasses by the FTIR experiment, on the one hand, and ECC experiment, on the other hand (Schneider et al.,

AMTD
5, 3431–3471, 2012

2008b). It is important to note that the scatter between FTIR and ECC concentrations decreases as the level of refinement of setups increases, especially in the troposphere and the tropopause region. Due to the reduction of the temperature error and the most realistic constraint, the setup C provides the FTIR profiles that best agree with the ECC sonde profiles.

The systematic discrepancies may be attributable to systematic ECC and FTIR errors caused, for instance, by uncertainties in the spectroscopic line parameters.

As addendum to the comparison to the ECC data Fig. 9 shows the comparison to the Brewer data that have been used in the Schneider et al. (2008a) paper. We observe that the scatter between the FTIR and Brewer ozone columns is significantly reduced (from 1.06 % to 0.71 %) as the FTIR setups become more refined, confirming the results of the FTIR-ECC comparison. Similar results were found for the comparison between FTIR and Izaña's surface data, i.e. the best agreement is obtained for the most sophisticated retrieval setup C. We find a mean bias and a scatter (1σ) of 20 % and 20 %, respectively, for the setup C and of 15 % and 23 %, respectively, for the configuration A. The respective systematic and random differences between the ECC sonde and Izaña's surface data are smaller (10 % and 15 %, respectively, recall Sect. 4.2). This is due to the FTIR's smoothing error.

6 Trends and seasonality

6.1 Ozone trends

Obtaining observational evidence of the projected trends in the vertical distribution of ozone is a difficult task. The trends are rather small and small instrumental drifts might cause artificial trends. Therefore, it is important to apply different measurement technics. Our study uses ECC sonde and ground-based FTIR.

Our time series are too short to employ multi-regression models (e.g. Reinsel et al., 2002), therefore, we use a bootstrap re-sampling method (Gardiner et al., 2008). This

AMTD
5, 3431–3471, 2012

method models the total variation in ozone by a function $F(t)$ and allows for separating the annual cycles from possible long-term trends:

$$F(t) = f_o + f_{\text{trend}}\, t + \sum_{i=1}^{p} [a_i \cos(\omega_i t) + b_i \sin(\omega_i t)] \quad (2)$$

where t is measured in years, f_o is a baseline constant, and f_{trend} the linear trend in change per year. The annual cycle is modeled in terms of a Fourier series where a_i and b_i are the parameters of the Fourier series to be determined and $\omega_i = 2\pi i/T$ with $T = 365.25$ days. We consider frequencies up to $3\,\text{yr}^{-1}$ ($p = 3$), since the third order Fourier series provided the best overall results (Gardiner et al., 2008; Vigouroux et al., 2008). Figure 11 shows the FTIR ozone time series (setup C) and the fitted function $F(t)$ for the different layers.

Although our bootstrap model does not capture atmospheric processes such as quasi-biennial oscillations (QBO) or solar cycle variations, they become a noise source in the linear trend determination, and, thus, feed into the uncertainties in the determined trends (Vigouroux et al., 2008). The significance of linear trends is estimated by the bootstrap method, which assumes that the residuals are Gaussian and uniform over the whole analyzed time period (Gardiner et al., 2008).

The observed trends from the FTIR time series slightly depend on the applied retrieval setup (Fig. 12). However, these differences are not significant and lie clearly within the 95 % confidence range (see error bars in Fig. 12). For all setups we observe significant negative linear trends between 1999 and 2010 for the tropopause region, while in the middle/upper stratosphere we document a stratospheric ozone increase. Nonetheless, in the troposphere we observe no significant trends with the setups retrieving the temperature profile (B and C), whereby the FTIR results do not allow making solid conclusions in this layer. The corrected ECC sonde time series confirms the FTIR trends, although the ECC trends are not significant (see Fig. 12). Note that the confidence range is given by 2σ standard deviations of the bootstrap re-sampled distributions.

AMTD
5, 3431–3471, 2012

Although a 12-yr time series is too short for trend studies, it is interesting that our results confirm those predicted by atmospheric chemical models. For example, Li et al. (2009) estimate that a decrease of ozone is to be expected in the lower stratosphere in the northern subtropical latitudes associated with the predicted increase in the stratospheric Brewer-Dobson circulation. An accelerated Brewer-Dobson circulation transports more ozone from tropics to the mid-high latitudes and could delay ozone recovery in the tropics and advanced ozone recovery in the extratropics. Furthermore, Li et al. (2009) show that the photochemical response to strong cooling induced by increasing greenhouse gases concentrations would lead to an upper stratospheric ozone increase. In addition, the leveling off of anthropogenic halogen components in the upper stratosphere since the mid-1990s has to be considered (WMO, 2007). Similar results were reported by WMO (2011).

It should be highlighted that for the upper stratosphere the quality of the FTIR time series has not been empirically validated due to the lack of respective ECC data. This is not satisfactory since at these altitudes the FTIR ozone data are very sensitive to ILS uncertainties and to measurement noise. Consequently, our upper stratospheric trend estimations should be treated with care, although the estimated upper stratospheric trends are consistent for all our setups and are supported by other experimental studies. For example, Steinbrecht et al. (2009) found that the upper stratospheric ozone (35–45 km) has been slightly increasing since the late 1990s at other NDACC sites (Mauna Loa, 19.5° N 155.6° E, and Table Mountain Observatories, 34.5° N 117.7° E), using satellite- and ground-based lidar measurements. This stratospheric ozone recovery has also been documented experimentally by FTIR records in northern subtropical, middle and polar latitudes (updated from Vigouroux et al., 2008 in WMO, 2011).

6.2 Ozone annual cycle

An ozone profile climatology, based on observations, is a useful tool to document the quality and consistency of the ozone estimates from climate models and from space-based sensors. Furthermore, it can be used as a priori information for ozone

AMTD
5, 3431–3471, 2012

retrieval algorithms. Thus, the ozone profile climatology presented here can be used as a benchmark at the subtropical North Atlantic region, where it is especially valuable due to the lack of high quality measurements of the ozone profiles.

The annual ozone cycles have been calculated by producing monthly averages applying the whole time series. Figure 13 shows the annual cycles for the FTIR data (setup A and C) and the corrected ECC sonde data. We observe that the agreement between the two techniques is rather satisfactory.

The annual cycle for the tropopause (2.37–10 km) reveals a maximum in spring-summer, which indicates the importance of photochemical production of tropospheric ozone. In the tropopause region (11–21 km) we observe a maximum in winter-spring and a minimum in summer and in early autumn, which is due to the large vertical shift of the subtropical tropopause altitude. In winter there is a mid-latitudinal tropopause and this layer belongs to the lower stratosphere, while in summer there is a tropical tropopause and this layer has rather upper tropospheric characteristics. The transformation from mid-latitudinal to tropical characteristics is also observed in the middle/upper stratosphere (22–29 km and 31–42 km). There we observe maximum ozone concentrations in summer-autumn when the tropical conditions prevail. In the middle stratosphere the FTIR system detects a maximum in spring that is not found in the ECC sonde annual cycle. This is due to the smoothing error: the FTIR ozone partial column in this layer contains information from the lower layers (11–21 km), where the spring maximum is due to the annual cycle in the tropopause altitude.

Note that applying different constraints and temperature retrievals do not significantly affect the ozone seasonality. Therefore, the least refined FTIR setup (setup A, "NDACC" approach) may be used to characterize properly the ozone annual cycle in these layers.

AMTD
5, 3431–3471, 2012

7 Conclusions

The FTIR technique can be a link between different measurement techniques, since it measures both high quality total column amounts and high quality profiles. In this work we have focused on the ozone profile time series, performing a theoretical and an empirical quality assessment. The latter is based on an extensive intercomparison study between FTIR and ECC sonde ozone profiles.

Before comparing the techniques, we have documented the consistency of these data. As a result, we find that the long-term quality of the ECC sonde data can be significantly improved by a correction that applies high quality total column measurements (in our study we apply Brewer total column data in order to remain independent from the FTIR data).

The intercomparison of techniques has shown that the FTIR system is able to capture adequately the ozone variability in the troposphere, tropopause region, and middle stratosphere. The agreement between the vertical ozone distribution obtained by the FTIR and the ECC sondes is very satisfactory. During the 12 yr period of 19990–2010 both techniques reveal very similar trends and annual seasonality. The differences in seasonality can be explained by the smoothing error of the FTIR ozone profiles.

The FTIR time series suggests that the long-term evolution of ozone concentrations is different at different altitude layers. We observe significant negative ozone trends in upper troposphere/lower stratosphere region and significant positive trends in the middle and upper stratosphere. Such trends are predicted by current climate models at the northern subtropical latitudes (Hegglin and Shepherd, 2009; Li et al., 2009). Despite this good agreement with the climate model predictions we have to be aware that a 12-yr time series might be too short for validating the models due to the large year-to-year variability of the stratospheric circulation (Weber et al., 2011). In addition, we would like to remark that high quality middle/upper stratospheric ozone measurements are very difficult. At these altitudes the FTIR ozone data are very sensitive to ILS uncertainties and to the measurement noise: a trend in the measurement noise will cause

AMTD
5, 3431–3471, 2012

a trend in the dof (see Fig. 3), which in its turn can generate an artificial trend in the ozone data. In this context super-sites like the Izaña Observatory, that concentrate numerous measurement techniques, are important. They allow for intercomparing the techniques, thereby documenting the long-term consistency of the profile datasets and their suitability for analyzing ozone trends. The fact that Izaña's ECC-sonde and FTIR time series show similar long-term trends adds a lot of confidence to our FTIR trend results.

Acknowledgements. Since 1999 the Izaña FTIR activities have been supported by different funding agencies: European Commission, European Space Agency, Deutsche Forschungsgemeinschaft, Deutsches Zentrum für Luft- und Raumfahrt, and the Ministerios de Ciencia e Innovación and Educación from Spain. Furthermore, the research leading to these results has received funding from the European Community's Seventh Framework Programme ([FP7/2007-2013]) under grant agreement no. 284421 (see Article II. 30. of the Grant Agreement). We are grateful to the Goddard Space Flight Center for providing the temperature and pressure profiles of the National Centers for Environmental Prediction. M. Schneider is supported by the European Research Council under the European Community's Seventh Framework Programme (FP7/2007-2013)/ERC Grant agreement no. 256961 and E. Sepúlveda enjoys a pre-doctoral fellowship from the Spanish Ministry of Education. Finally, the authors would like thank Carlos Marrero and Pedro M. Romero for their useful comments.

References

Barret, B., Maziére, M. D., and Demoulin, P.: Retrieval and characterization of ozone profiles from solar infrared spectra at the Jungfraujoch, J. Geophys. Res., 107, 4788–4803, 2002. 3436

Calisesi, Y., Soebijanta, V., and van Oss, R.: Regridding of remote soundings: Formulation and application to ozone profile comparison, J. Geophys. Res., 110, D23306, doi:10.1029/2005JD006122, 2005. 3444

Gardiner, T., Forbes, A., de Mazière, M., Vigouroux, C., Mahieu, E., Demoulin, P., Velazco, V., Notholt, J., Blumenstock, T., Hase, F., Kramer, I., Sussmann, R., Stremme, W., Mellqvist, J., Strandberg, A., Ellingsen, K., and Gauss, M.: Trend analysis of greenhouse gases over

AMTD
5, 3431–3471, 2012

Europe measured by a network of ground-based remote FTIR instruments, Atmos. Chem. Phys., 8, 6719–6727, doi:10.5194/acp-8-6719-2008, 2008. 3445, 3446
Hase, F., Blumenstock, T., and Paton-Walsh, C.: Analysis of the instrumental line shape of high-resolution Fourier transform IR spectrometers with gas cell measurements and new retrieval software, Appl. Optics, 38, 3417–3422, 1999. 3440
Hase, F., Hanningan, J. W., Coffey, M. T., Goldman, A., Höfner, M., Jones, N. B., Rinsland, C. P., and Wood, S. W.: Intercomparison of retrieval codes used for the analysis of high-resolution ground-based FTIR measurements, J. Quant. Spectrosc. Ra., 87, 25–52, 2004. 3436, 3438
Hegglin, M. I. and Shepherd, T. G.: Large climate-induced changes in ultraviolet index and stratosphere-to troposphere ozone flux, Nat. Geosci., 2, 687–691, doi:10.1038/NGEO604, 2009. 3433, 3449
Kurylo, M. J. and Zander, R.: The NDSC-Its status after 10 years of operation, in: Proceedings of XIX Quadrennian Ozone Symposium, Hokkaaido University, Sapporo, Japan,167–168, 2000. 3433
Lanzante, J. R.: Resistant, robust and non-parametric techniques or the anayliss of climate data: theory and examples, including applications to historical radiosonde station data, Int. J. Climatol., 16, 1197–1226, 1996. 3442
Li, F., Stolarski, R. S., and Newman, P. A.: Stratospheric ozone in the post-CFC era, Atmos. Chem. Phys., 9, 2207–2213, doi:10.5194/acp-9-2207-2009, 2009. 3433, 3447, 3449
Nair, P. J., Godin-Beekmann, S., Pazmiño, A., Hauchecorne, A., Ancellet, G., Petropavlovskikh, I., Flynn, L. E., and Froidevaux, L.: Coherence of long-term stratospheric ozone vertical distribution time series used for the study of ozone recovery at a northern mid-latitude station, Atmos. Chem. Phys., 11, 4957–4975, doi:10.5194/acp-11-4957-2011, 2011. 3444
Redondas, A. and Cede, A.: Brewer algorithm sensitiviy analysis, in: Sauna Workshop, Puerto de la Cruz, Tenerife, 2006. 3442
Reinsel, G. C., Weatherhead, E. C., Tiao, G. C., Miller, A. J., Nagatani, R. M., Wuebbles, D. J., and Flynn, L. E.: On detection of turnaround and recovery in trend for ozone, J. Geophys. Res., 107, 4078–4090, 2002. 3445
Rodgers, C.: Inverse Methods for Atmospheric Sounding: Theory and Praxis, World Scientific Publishing Co., Singapore, 2000. 3436, 3438
Romero, P. M., Marrero, C. L., Alonso-Péerez, S., Cuevas, E., and Afonso, S.: Una climatología del agua precipitable en la región subtropical sobre la Isla de Tenerife, vol. NTD CIAI-6, NIPO: 281-12-007-5, Servicio de Publicaciones de la AEMET, Madrid, Spain, 2011. 3443

AMTD
5, 3431–3471, 2012

Rothman, L. S., Gordon, I. E., Barbe, A., Benner, D. C., Bernath, P. F., Birk, M., Boudon, V., Brown, L. R., Campargue, A., Champion, J.-P., Chance, K., Coudert, L. H., Dana, V., Devi, V. M., Fally, S., Flaud, J.-M., Gamache, R. R., Goldmanm, A., Jacquemart, D., Kleiner, I., Lacome, N., Lafferty, W., Mandin, J.-Y., Massie, S. T., Mikhailenko, S. N., Miller, C. E., Moazzen-Ahmadi, N., Naumenko, O. V., Nikitin, A. V., Orphal, J., Perevalov, V. I., A. Perrini, A. P.-C., Rinsland, C. P., Rotger, M., Šimečková, M., Smith, M. A. H., Sung, K., Tashkun, S. A., Tennyson, J., Toth, R. A., Vandaele, A. C., and VanderAuwera, J.: The HITRAN 2008 Molecular Spectroscopic Database, J. Quant. Spectrosc. Ra., 110, 533–572, 2009. 3436

Schneider, M. and Hase, F.: Technical Note: Recipe for monitoring of total ozone with a precision of around 1 DU applying mid-infrared solar absorption spectra, Atmos. Chem. Phys., 8, 63–71, doi:10.5194/acp-8-63-2008, 2008. 3433, 3436

Schneider, M., Hase, F., and Blumenstock, T.: Ground-based remote sensing of HDO/H_2O ratio profiles: introduction and validation of an innovative retrieval approach, Atmos. Chem. Phys., 6, 4705–4722, doi:10.5194/acp-6-4705-2006, 2006. 3436

Schneider, M., Redondas, A., Hase, F., Guirado, C., Blumenstock, T., and Cuevas, E.: Comparison of ground-based Brewer and FTIR total column O_3 monitoring techniques, Atmos. Chem. Phys., 8, 5535–5550, doi:10.5194/acp-8-5535-2008, 2008a. 3433, 3442, 3445

Schneider, M., Hase, F., Blumenstock, T., Redondas, A., and Cuevas, E.: Quality assessment of O_3 profiles measured by a state-of-the-art ground-based FTIR observing system, Atmos. Chem. Phys., 8, 5579–5588, doi:10.5194/acp-8-5579-2008, 2008b. 3433, 3436, 3444

Sepúlveda, E., Schneider, M., Hase, F., García, O. E., Gomez-Pelaez, A., Dohe, S., Blumenstock, T., and Guerra, J. C.: Long-term validation of total and tropospheric column-averaged CH_4 mole fractions obtained by mid-infrared ground-based FTIR spectrometry, Atmos. Meas. Tech. Discuss., 5, 1381–1430, doi:10.5194/amtd-5-1381-2012, 2012. 3435

Smit, H. G. J., Straeter, W., Johnson, B. J., Oltmans, S. J., Davies, J., Tarasick, D. W., Hoegger, B., Stubi, R., Schmidlin, F. J., Northam, T., amd J. C. Witte, A. M. T., Boyd, I., and Posny, F.: Assessment of the performance of ECC-ozonesondes under quasi-flight conditions in the environmental simulation chamber: Insights from the Juelich Ozone Sonde Intercomparison Experiment (JOSIE), J. Geophys. Res., 112, D19306, doi:10.1029/2006JD007308, 2007. 3435, 3442, 3444

Steinbrecht, W., Claude, H., Schönenborn, F., McDermid, I. S., Leblanc, T., Godin-Beekmann, S., Keckhut, P., Hauchecorne, J. A. E. V. G., Swart, D. P. J., Bodeker, G. E., Parrish, A., Boyd, I. S., Kämpfer, N., Hocke, K., Stolarski, R. S., Frith, S. M., Thomason, L. W., Remsberg, E. E.,

AMTD
5, 3431–3471, 2012

Savigny, C. V., Rozanov, A., and Burrows, J. P.: Ozone and temperature trends in the upper stratosphere at five stations of the Network for the Detection of Atmospheric Composition Change, Int. J. Remote Sens., 30, 3875–3886, 2009. 3447

Viatte, C., Schneider, M., Redondas, A., Hase, F., Eremenko, M., Chelin, P., Flaud, J.-M., Blumenstock, T., and Orphal, J.: Comparison of ground-based FTIR and Brewer O_3 total column with data from two different IASI algorithms and from OMI and GOME-2 satellite instruments, Atmos. Meas. Tech., 4, 535–546, doi:10.5194/amt-4-535-2011, 2011. 3433

Vigouroux, C., De Mazière, M., Demoulin, P., Servais, C., Hase, F., Blumenstock, T., Kramer, I., Schneider, M., Mellqvist, J., Strandberg, A., Velazco, V., Notholt, J., Sussmann, R., Stremme, W., Rockmann, A., Gardiner, T., Coleman, M., and Woods, P.: Evaluation of tropospheric and stratospheric ozone trends over Western Europe from ground-based FTIR network observations, Atmos. Chem. Phys., 8, 6865–6886, doi:10.5194/acp-8-6865-2008, 2008. 3433, 3446, 3447

Weatherhead, E. and Andersen, S.: The search for signs of recovery of the ozone layer, Nature, 441, 39–45, 2006. 3433

Weber, M., Dikty, S., Burrows, J. P., Garny, H., Dameris, M., Kubin, A., Abalichin, J., and Langematz, U.: The Brewer-Dobson circulation and total ozone from seasonal to decadal time scales, Atmos. Chem. Phys., 11, 11221–11235, doi:10.5194/acp-11-11221-2011, 2011. 3449

WMO: Scientific Assessment of Ozone Depletion: 2006, Global Ozone Research and Monitoring Project-Report No. 50, World Meteorological Organization, Geneva, Switzerland, 2007. 3447

WMO: Scientific Assessment of Ozone Depletion: 2010, Global Ozone Research and Monitoring Project-Report No. 2, World Meteorological Organization, Geneva, Switzerland, 2011. 3447

Zellweger, C., Klausen, J., Buchmann, B., and Scheel, H.-E.: System and Performance Audit of Surface Ozone, Carbon Monoxide, Methane and Nitrous Oxide at the Global GAW Station Izaña, Tech. rep., WCC-EMPA Report 09/1, 2009. 3435

AMTD
5, 3431–3471, 2012

Table 1. Description of FTIR ozone retrieval setups. Note that the level of refinement increases from the setup A to the setup C. [1]Four temperature microwindows (MW) with isolated CO_2 signatures [cm^{-1}]: 962.80–963.80, 964.25–965.25, 967.20–968.20, 968.60–969.60.

Retrieval Setup	A: "NDACC"	B + Temperature	C + (TP → OE)
MW [cm^{-1}]	1000–1005	1000–1005 + Temp. MW[1]	1000–1005 + Temp. MW[1]
Interfering species	$^{666}O_3$, $^{686}O_3$, $^{668}O_3$ H_2O, CO_2, C_2H_4	$^{666}O_3$, $^{686}O_3$, $^{668}O_3$ H_2O, CO_2, C_2H_4	$^{666}O_3$, $^{686}O_3$, $^{668}O_3$ H_2O, CO_2, C_2H_4
Logarithmic scale	Yes	Yes	Yes
Temp. retrieval	No	Yes	Yes
Int.-Spec. Const.	No	No	Yes
Inversion method	Tikhonov-Phillips (TP) with slope constraint (TP1)	Tikhonov-Phillips (TP) with slope constraint (TP1)	Optimal Estimation (OE) with $\mathbf{S}_a$ from Tfe's ECC sondes

AMTD
5, 3431–3471, 2012

Table 2. Mean (M) and standard deviation (σ) of the dof time series of the retrieved ozone obtained from the spectrometer 120/5HR for all setups. These values are shown for each layer (2.37–10 km, 11–21 km, 22–29 km, 31–42 km) and for the total column (2.37–120 km). The standard error of the mean, SEM, is lower than 0.01 for all setups and layers (not shown).

Layer	Retrieval Setup		
[km]	A M, σ	B M, σ	C M, σ
2.37–10	0.87, 0.05	0.93, 0.04	1.04, 0.06
11–21	0.81, 0.09	0.92, 0.07	1.21, 0.11
22–29	1.01, 0.06	1.06, 0.05	1.02, 0.05
31–42	0.92, 0.04	0.94, 0.04	0.86, 0.05
2.37–120	3.84, 0.23	4.10, 0.14	4.20, 0.17

AMTD
5, 3431–3471, 2012

Table 3. Assumed experimental and temperature uncertainties.

Error Source	Uncertainty
Modulation Eff.	1 %
Phase Error	0.01 rad
Baseline Offset	0.1 %
Temperature profile	2 K below 50 km 5 K above 50 km
Line Of Sight (LOS)	0.1°
Solar lines (intensity and scale)	1 %, 10^{-6}
Spectroscopic parameters	1 %

AMTD
5, 3431–3471, 2012

Table 4. Estimated random errors relative to actual ozone partial columns [%] for the Izaña spectrometer 120/5HR for all setups and for the different layers.

Layer [km]	Retrieval Setup		
	A TPE[1], SE[2], **TRE**[3]	B TPE[1], SE[2], **TRE**[3]	C TPE[1], SE[2], **TRE**[3]
2.37–10	0.9, 9.9, **9.9**	1.0, 9.6, **9.6**	1.2, 7.1, **7.2**
11–21	1.0, 5.3, **5.4**	0.9, 4.5, **4.5**	0.9, 3.5, **3.6**
22–29	2.3, 2.8, **3.6**	0.9, 2.9, **3.0**	0.8, 2.8, **2.9**
31–42	3.7, 3.6, **5.1**	2.2, 3.4, **4.0**	2.2, 5.4, **5.8**

[1] TPE [%]: Total Parameter Error due to input parameters and measurement noise; [2] SE [%]: Smoothing Error; [3] TRE [%, in bold]: Total Random Error.

AMTD
5, 3431–3471, 2012

Table 5. Statistics of coincident measurements from the IFS 120/5HR and IFS 120M ozone partial columns for each setup and layer ($N = 19$).

Layer [km]	Retrieval Setup		
	A $M \pm \text{SEM}^1$, σ^2, S^3, R^4	B $M \pm \text{SEM}^1$, σ^2, S^3, R^4	C $M \pm \text{SEM}^1$, σ^2, S^3, R^4
2.37−−10	−1.67 ± 0.45, 1.98, 1.01 ± 0.00, 0.99	+1.67 ± 0.53, 2.32, 0.98 ± 0.01, 0.99	−0.26 ± 0.46, 2.00, 1.00 ± 0.00, 0.99
11−−21	+4.03 ± 0.44, 1.91, 0.95 ± 0.00, 0.99	+4.33 ± 0.50, 2.17, 0.96 ± 0.00, 0.99	+5.27 ± 0.49, 2.12, 0.95 ± 0.00, 0.99
22−−29	−6.25 ± 0.44, 1.90, 1.07 ± 0.00, 0.96	−3.99 ± 0.39, 1.70, 1.04 ± 0.00, 0.97	−3.74 ± 0.34, 1.49, 1.04 ± 0.00, 0.97
31−−42	−1.08 ± 0.81, 3.52, 1.01 ± 0.01, 0.71	+2.99 ± 0.67, 2.91, 0.97 ± 0.01, 0.80	+4.07 ± 0.56, 2.44, 0.96 ± 0.01, 0.83

[1] $M \pm \text{SEM}$ [%]: mean and standard error of the mean of relative differences (120M-120/5HR)/120/5HR; [2] σ [%]: standard deviation of relative differences; [3] S: slope of the linear regression trough origin; [4] R: correlation coefficient of the linear fit.

AMTD
5, 3431–3471, 2012

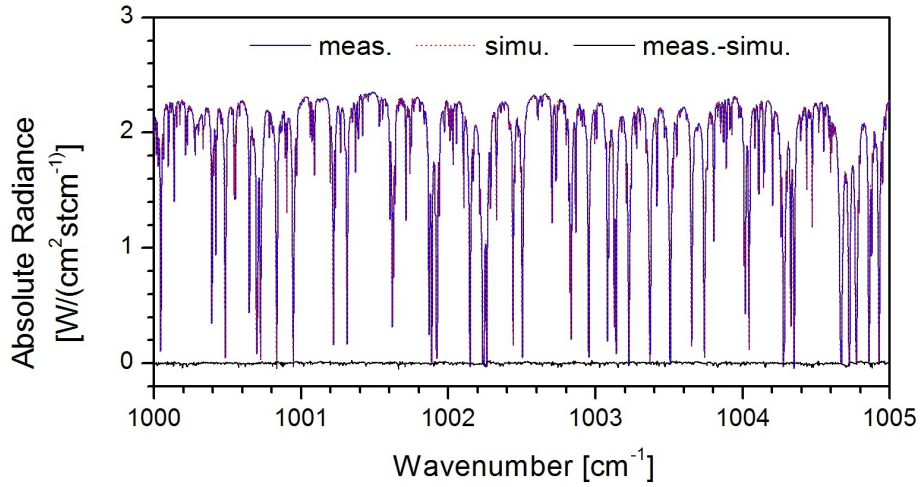

Fig. 1. Spectral microwindow applied for ozone retrievals.

AMTD
5, 3431–3471, 2012

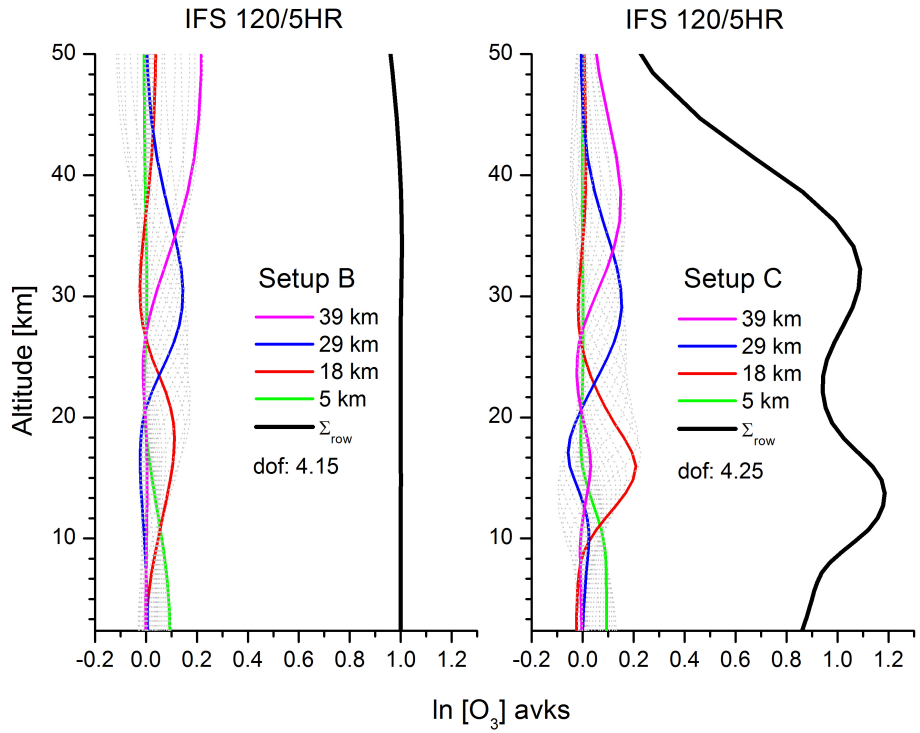

Fig. 2. FTIR averaging kernels, avks, for retrieved ozone values using the setup B (left panel) and C (right panel), expressed as ln[O_3], for the Izaña spectrometer 120/5HR. Σ_{row} (black line) is the total sensitivity of FTIR system and dof is the degrees of freedom for signal.

AMTD
5, 3431–3471, 2012

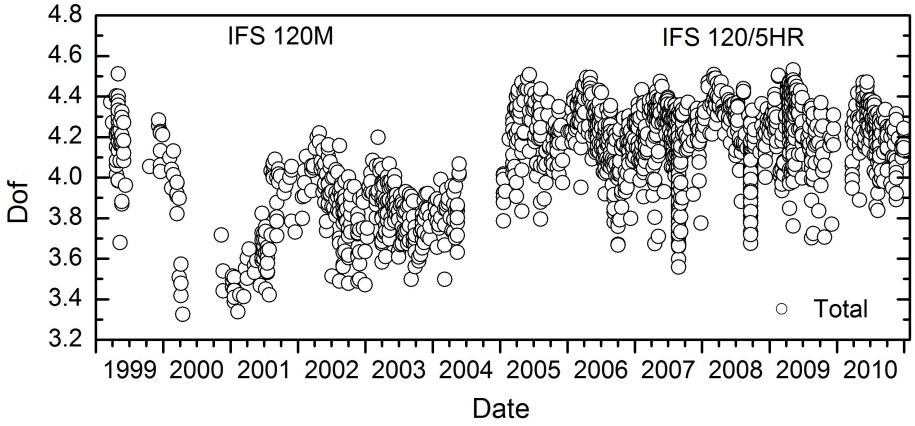

Fig. 3. Time series of total dof of retrieved ozone values using the setup C for the whole FTIR time series between 1999 and 2010 (number of data, *N*, is 1887).

AMTD
5, 3431–3471, 2012

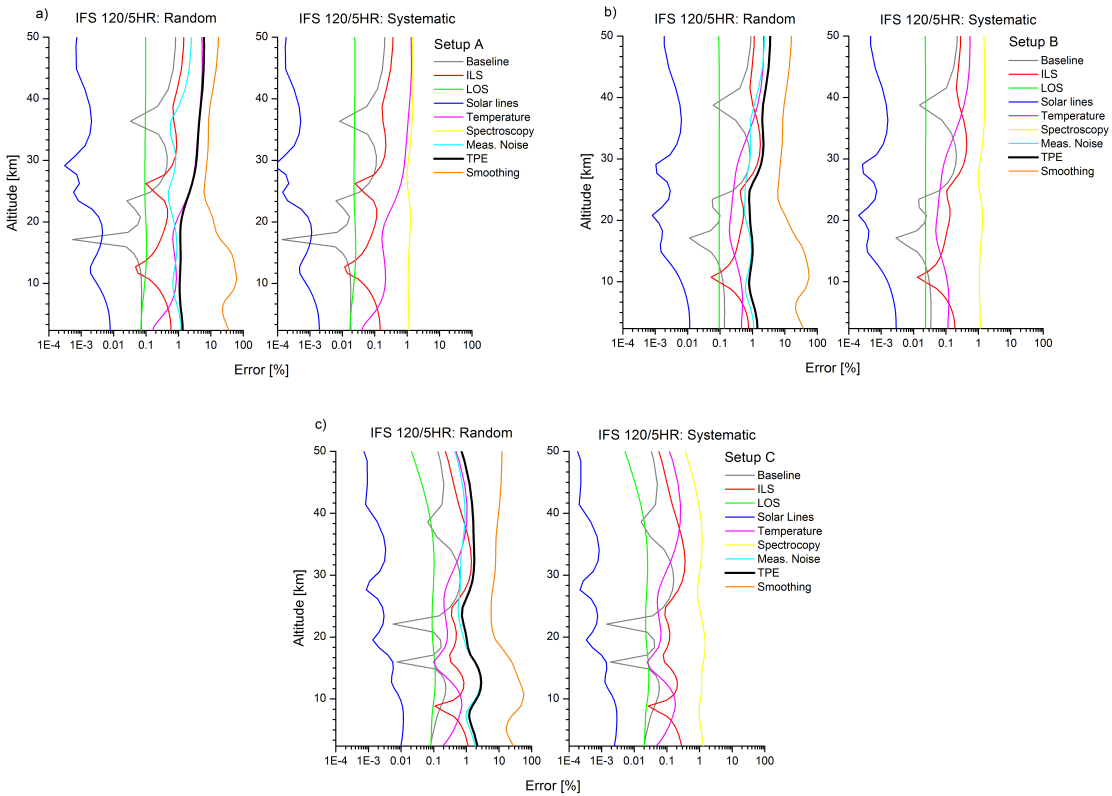

Fig. 4. VMR random and systematic errors relative to actual ozone VMR profiles [%] for the Izaña spectrometer 120/5HR for the setups A **(a)**, B **(b)** and C **(c)**. ILS means the joint error due to the modulation efficiency and phase error uncertainties and TPE (Total Parameter Error, black line) is the sum of all random errors except for smoothing error.

AMTD
5, 3431–3471, 2012

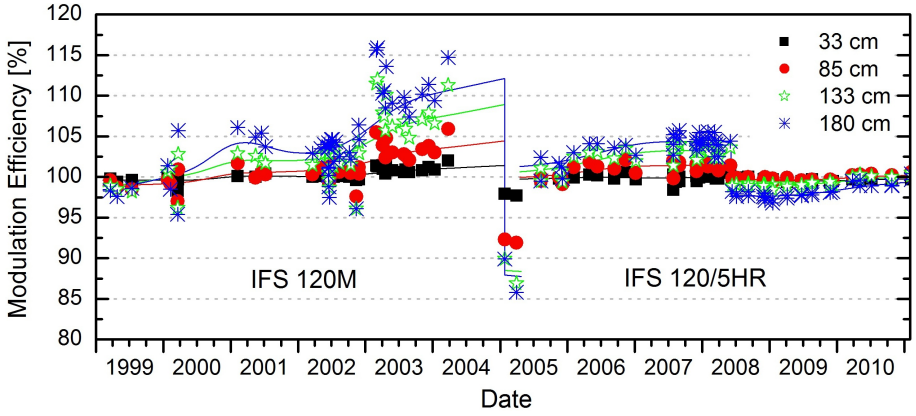

Fig. 5. Times series of the modulation efficiency [%] at different optical path differences (OPD) for the Izaña spectrometers. Individual data points indicate individual cell measurements. The lines are the smoothed efficiency curves used during the FTIR retrievals. Black at 38 cm, red at 85 cm, green at 133 cm and blue at 180 cm.

AMTD
5, 3431–3471, 2012

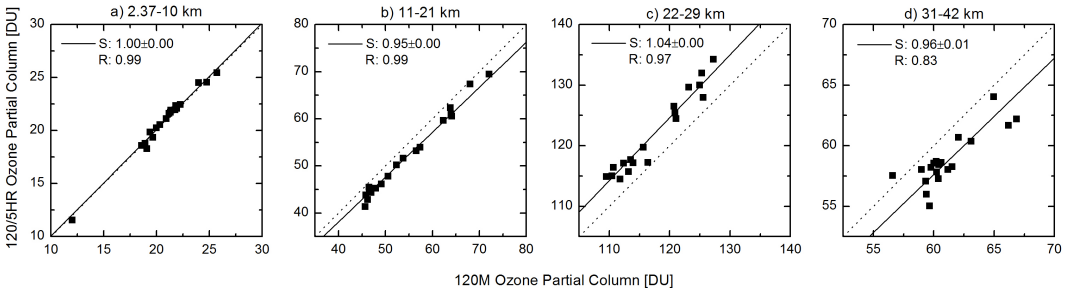

Fig. 6. Comparison between the IFS 120/5HR and IFS 120M ozone partial columns [DU] for the 120M-120/5HR coincidences during April and May 2005 ($N = 19$): **(a)** 2.37–10 km, **(b)** 11–21 km and **(c)** 22–29 km and **(d)** 31–42 km. The black solid lines are the linear regression lines through origin, whose parameters are shown in the legend (S is the slope of regression fit and R the correlation coefficient). The dotted lines are the diagonals.

AMTD
5, 3431–3471, 2012

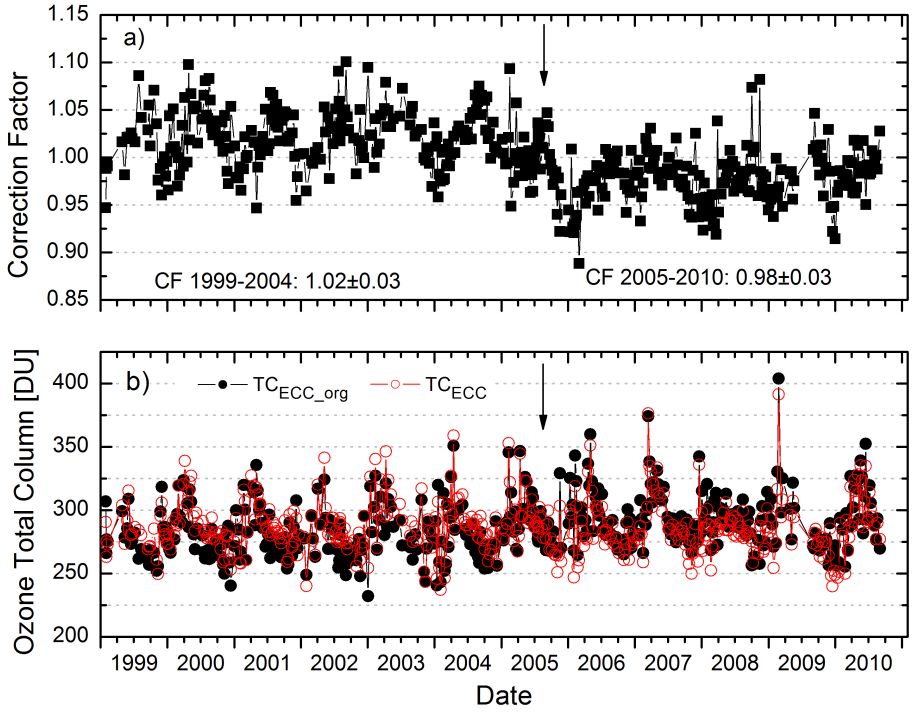

Fig. 7. Time series of correction factor (CF, according to Eq. 1) at the Izaña Observatory **(a)** and of ozone total column from ECC sondes without correction (TC_{ECC_org}) and corrected by the daily CF Brewer/ECC_org (TC_{ECC}) **(b)**. The mean correction factor for the periods 1999–2004 and 2005–2010 is also shown. The black arrows indicate the change-point date.

AMTD
5, 3431–3471, 2012

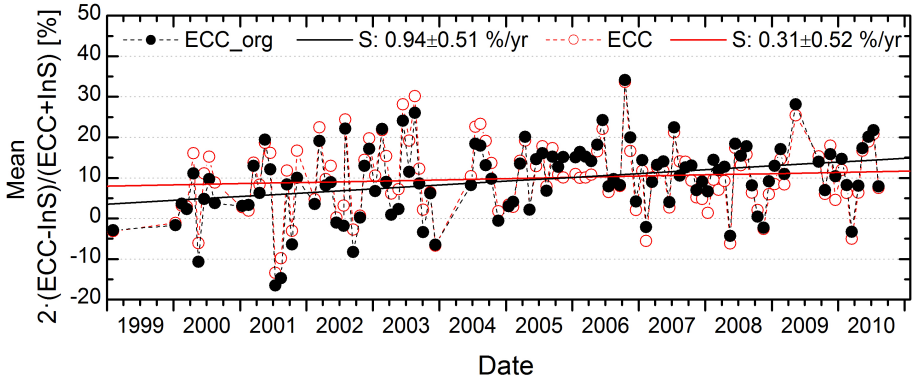

Fig. 8. Monthly mean time series of the relative differences [%] between the ozone VMR from the ECC sonde data (corrected, ECC, and not corrected by the daily CF, ECC_org,) at Izaña's altitude and surface data ($N = 112$). The solid lines are the linear regression lines of the least square fits. The slopes and the 95 % confidence ranges ($\pm 2\sigma$) are shown in the legend (S).

AMTD
5, 3431–3471, 2012

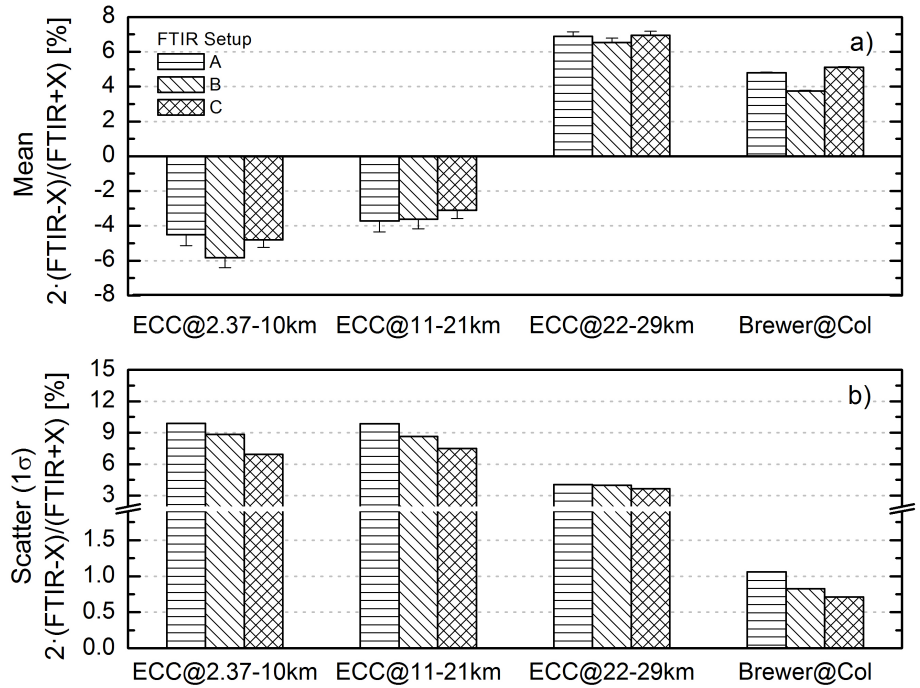

Fig. 9. Relative differences [%] between the ozone partial columns (2.37–10 km, 11–21 km and 22–29 km) calculated from the ECC sonde and from the different FTIR setups: **(a)** mean values (error bars indicate the standard error of the mean) and **(b)** scatter or standard deviation (1σ). It is also shown the differences between the FTIR and Brewer ozone columns. *X* means the ECC or Brewer data.

AMTD
5, 3431–3471, 2012

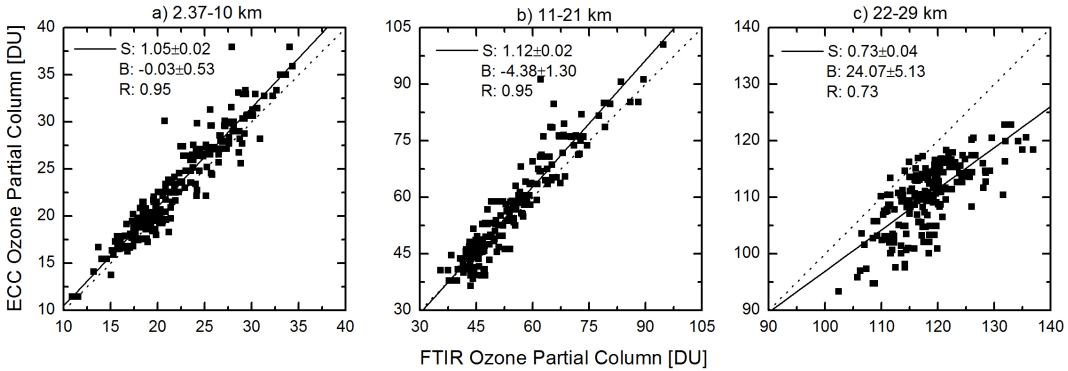

Fig. 10. Comparison between the ozone partial columns from FTIR (setup C) and ECC sonde data ($N = 243$): **(a)** 2.37–10 km, **(b)** 11–21 km and **(c)** 22–29 km. The black solid lines are the linear regression line of the least square fits, whose parameters are shown in the legend (S and B are the slope and the bias of the regression fit respectively and R the correlation coefficient). The dotted lines are the diagonals.

AMTD
5, 3431–3471, 2012

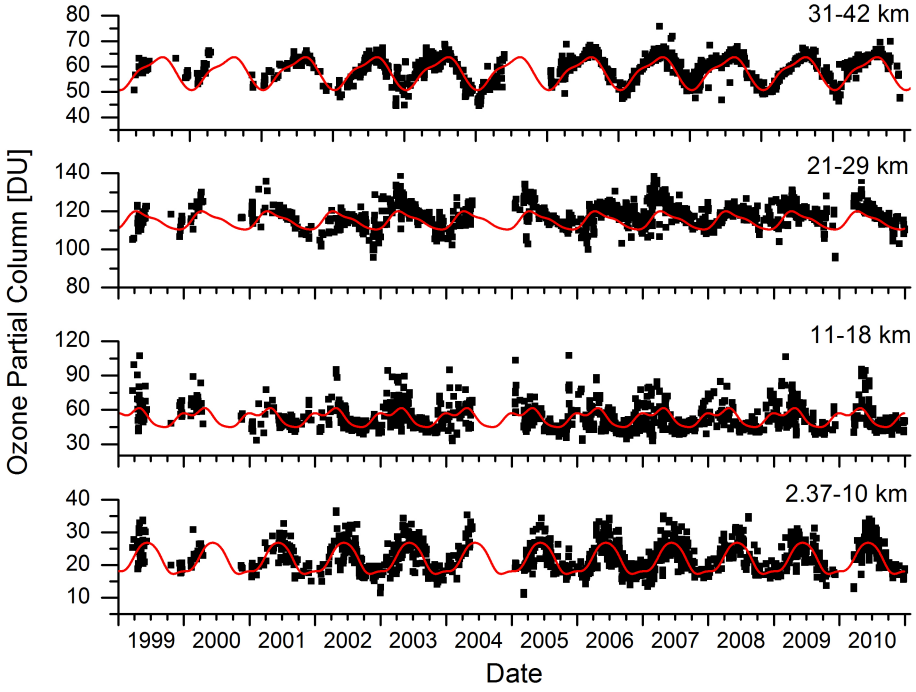

Fig. 11. Time series of FTIR ozone partial columns [DU] (setup C) for the different layers. Black dots: individual measurements ($N = 1887$); Red lines: annual cycle according to Eq. (2).

AMTD
5, 3431–3471, 2012

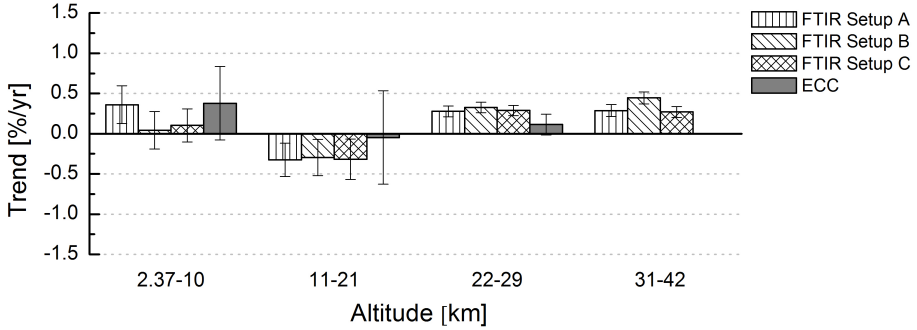

Fig. 12. Linear trends (change/10a, % yr^{-1}) between 1999 and 2010 for the FTIR ($N = 1887$) and the corrected ECC sonde ($N = 459$) datasets. The error bars indicate the 95 % confidence ranges ($\pm 2\sigma$).

AMTD
5, 3431–3471, 2012

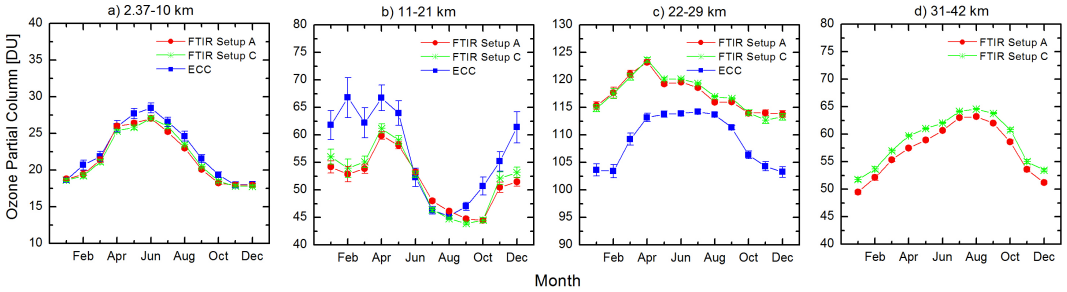

Fig. 13. Annual cycle of the ozone partial columns [DU] obtained from the FTIR (setup A and C) and the corrected ECC sonde data: **(a)** 2.37–10 km, **(b)** 11–21 km, **(c)** 22–29 km and **(d)** 31–42 km. The error bars indicate the standard error of the mean value.

AMTD
5, 3431–3471, 2012